Article

Complexation-Induced Transition of Nanorod to Network Aggregates: Alternate Porphyrin and Cyclodextrin Arrays

Yu Liu, Chen-Feng Ke, Heng-Yi Zhang, Jie Cui, and Fei Ding

J. Am. Chem. Soc., **2008**, 130 (2), 600-605 • DOI: 10.1021/ja075981v

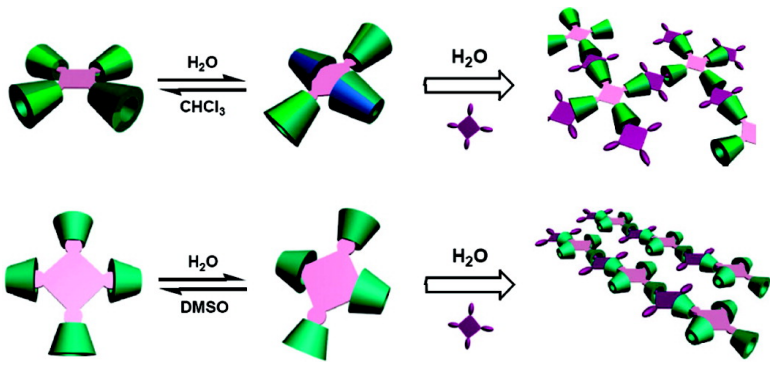

More About This Article

Additional resources and features associated with this article are available within the HTML version:

- Supporting Information
- Links to the 1 articles that cite this article, as of the time of this article download
- Access to high resolution figures
- Links to articles and content related to this article
- Copyright permission to reproduce figures and/or text from this article

View the Full Text HTML

J|A|C|S
ARTICLES
Published on Web 12/21/2007

Complexation-Induced Transition of Nanorod to Network Aggregates: Alternate Porphyrin and Cyclodextrin Arrays

Yu Liu,* Chen-Feng Ke, Heng-Yi Zhang, Jie Cui, and Fei Ding

Department of Chemistry, State Key Laboratory of Elemento-Organic Chemistry, Nankai University, Tianjin, 300071, P. R. China

Received August 8, 2007; E-mail: yuliu@nankai.edu.cn

Abstract: Tetrakis(permethyl-β-cyclodextrin)-modified zinc(II) porphyrin (**1**) and tetra(β-cyclodextrin)-modified zinc(II) porphyrin (**2**) were synthesized via "click chemistry". Intermolecular inclusion complexation of these structurally similar **1** and **2** with tetrasodium tetraphenylporphyrintetrasulfonate (**3**) led to formation of two distinctly different nanoarchitectures with alternate porphyrin and cyclodextrin arrays, which were proven to be network and nanorod aggregates, respectively, by using transmission electron microscopy, atomic force microscopy, and scanning electron microscopy. From the results of comparative studies in different solutions, we elucidated the mechanisms that result in nanorod to network aggregates transition, concluding that the complexation strength of porphyrin with cyclodextrin is a crucial factor to activate the potential binding sites of a molecular building block.

Introduction

Self-assembly processes are ubiquitous in chemistry, materials science, and biology. The morphology of the assembly is usually determined by the structure of the individual components.[1] Therefore, the design of molecular building blocks and binding motif that organize themselves into desired patterns and functions is the key to the application of self-assembly.[2] On the other hand, a functional molecular building block employed in supramolecular chemistry usually possesses an invariable shape with unambiguous functional binding sites, which lead them to a supramolecular assembly with a fixed pattern. In biology, stem cells can differentiate to divergent cell types that make up the organism when the right signals are provided. That is, stem cells have the potential to develop into mature cells that have characteristic shapes and specialized functions. Thus, the design of functional molecular building blocks which are similar to stem cells remains challenging.

Porphyrins have been widely used as functional building blocks in supramolecular chemistry because of their photochemical properties,[3] the ability to be used as donor/accepter ability in electron or energy transfer process,[4] and so on.[5] In particular, the combination of porphyrins and cyclodextrins (CDs) becomes an important topic for designing functional supramolecular assemblies,[6,7] and the binding behavior, enzyme mimics, and energy/electron transfer abilities of porphyrin-CD conjugates have been investigated.[8] Herein, we report the construction of two supramolecular nanoarchitectures whose aggregation patterns are controlled by selectively activating the potential binding sites of the molecular building blocks. Using transmission electron microscopy (TEM), atomic force microscopy (AFM), and scanning electron microscopy (SEM), we will show that the constructed nanorods or network aggregates are formed by the noncovalent interactions of *meso*-tetraphenylporphyrin-4,4′,4″,4‴-tetrasulfonic acid tetrasodium salt (**3**) with porphyrin-β-CD or porphyrin-permethyl-β-CD conjugates, and also that the morphology switching is controlled in a predictable fashion by the complexation strength of porphyrins with CDs.

(1) Whitesides, G. M.; Simanek, E. E.; Gorman, C. B. In *Chemical Synthesis: Gnosis to Prognosis;* Chatgilialoglu, C., Snieckus, V., Eds.; NATO Advanced Study Institute Series 320; Kluwer: Dordrecht, The Netherlands, 1996; pp 565−588.
(2) Whitesides, G. M.; Grzybowski, B. *Science* **2002**, *295*, 2418−2421.
(3) (a) Sessler, J. L.; Wang, B.; Harriman, A. *J. Am. Chem. Soc.* **1995**, *117*, 704−714. (b) Sugou, K.; Sasaki, K.; Kitajima, K.; Iwaki, T.; Kuroda, Y. *J. Am. Chem. Soc.* **2002**, *124*, 1182−1183.
(4) (a) Haycock, R. A.; Yartsev, A.; Michelsen, U.; Sundström, V.; Hunter, C. A. *Angew. Chem., Int. Ed.* **2000**, *39*, 3616−3619. (b) Choi, M.-S.; Aida, T.; Yamazaki, T.; Yamazaki, I. *Chem.−Eur. J.* **2002**, *8*, 2667−2678. (c) Prathapan, S.; Johnson, T. E.; Lindsey, J. S. *J. Am. Chem. Soc.* **1993**, *115*, 7519−7520.
(5) (a) Choi, M.-S.; Yamazaki, T.; Yamazaki, I.; Aida, T. *Angew. Chem., Int. Ed.* **2004**, *43*, 150−158. (b) Alessio, E.; Iengo, E.; Marzilli, L. G. *Supramol. Chem.* **2002**, *14*, 103−120.
(6) (a) Dai, X.-H.; Dong, C.-M.; Fa, H.-B.; Yan, D.-Y.; Wei, Y. *Biomacromolecules* **2006**, *7*, 3527−3533. (b) Kano, K.; Kitagishi, H.; Mabuchi, T.; Kodera, M.; Hirota, S. *Chem. Asian J.* **2006**, *1*, 358−366. (c) Kano, K.; Nishiyabu, R.; Asada, T.; Kuroda, Y. *J. Am. Chem. Soc.* **2002**, *124*, 9937−9944. (d) Deng, W.; Onji, T.; Yamaguchi, H.; Ikedab, N.; Harada, A. *Chem. Commun.* **2006**, 4212−4214. (e) Lang, K.; Mosinger, J.; Wagnerová, D. M. *Coord. Chem. Rev.* **2004**, *248*, 321−350. (f) Mulder, A.; Jukovic, A.; van Leeuwen, F. W. B.; Kooijman, H.; Spek, A. L.; Huskens, J.; Reinhoudt, D. N. *Chem.−Eur. J.* **2004**, *10*, 1114−1123.
(7) (a) Sasaki, K.; Nakagawa, H.; Zhang, X.-Y.; Sakurai, S.; Kano, K.; Kuroda, Y. *Chem. Commun.* **2004**, 408−409. (b) Kano, K.; Kitagishi, H.; Dagallier, C.; Kodera, M.; Matsuo, T.; Hayashi, T.; Hisaeda, Y.; Hirota, S. *Inorg. Chem.* **2006**, *45*, 4448−4460. (c) Kano, K.; Kitagishi, H.; Tamura, S.; Yamada, A. *J. Am. Chem. Soc.* **2004**, *126*, 15202−15210. (d) Venema, F.; Rowan, A. E.; Nolte, R. J. M. *J. Am. Chem. Soc.* **1996**, *118*, 257−258. (e) Kano, K.; Ishida, Y. *Angew. Chem., Int. Ed.* **2007**, *46*, 727−730. (f) Kano, K.; Kitagishi, H.; Kodera, M.; Hirota, S. *Angew. Chem., Int. Ed.* **2005**, *44*, 435−438.
(8) (a) Kuroda, Y.; Hiroshige, T.; Sera, T.; Shiroiwa, Y.; Tanaka, H.; Ogoshi, H. *J. Am. Chem. Soc.* 1**989**, *111*, 1912−1913. (b) Kuroda, Y.; Ito, M.; Sera, T.; Ogoshi, H. *J. Am. Chem. Soc.* **1993**, *115*, 7003−7004. (c) Kano, K.; Nishiyabu, R.; Yamazaki, T.; Yamazaki, I. *J. Am. Chem. Soc.* **2003**, *125*, 10625−10634. (d) Breslow, R.; Zhang, X.; Xu, R.; Maletic, M.; Merger, R. *J. Am. Chem. Soc.* **1996**, *118*, 11678−11679. (e) Breslow, R.; Zhang, X.; Huang, Y. *J. Am. Chem. Soc.* **1997**, *119*, 4535−4536. (f) Carofiglio, T.; Fornasier, R.; Lucchini, V.; Simonato, L.; Tonellato, U. *J. Org. Chem.* **2000**, *65*, 9013−9021. (g) Leng, X.-B.; Choi, C.-F.; Lo, P.-C.; Ng, D. K. P. *Org. Lett.* **2007**, *9*, 231−234.

10.1021/ja075981v CCC: $40.75

Scheme 1. Synthesis of **1** and **2**

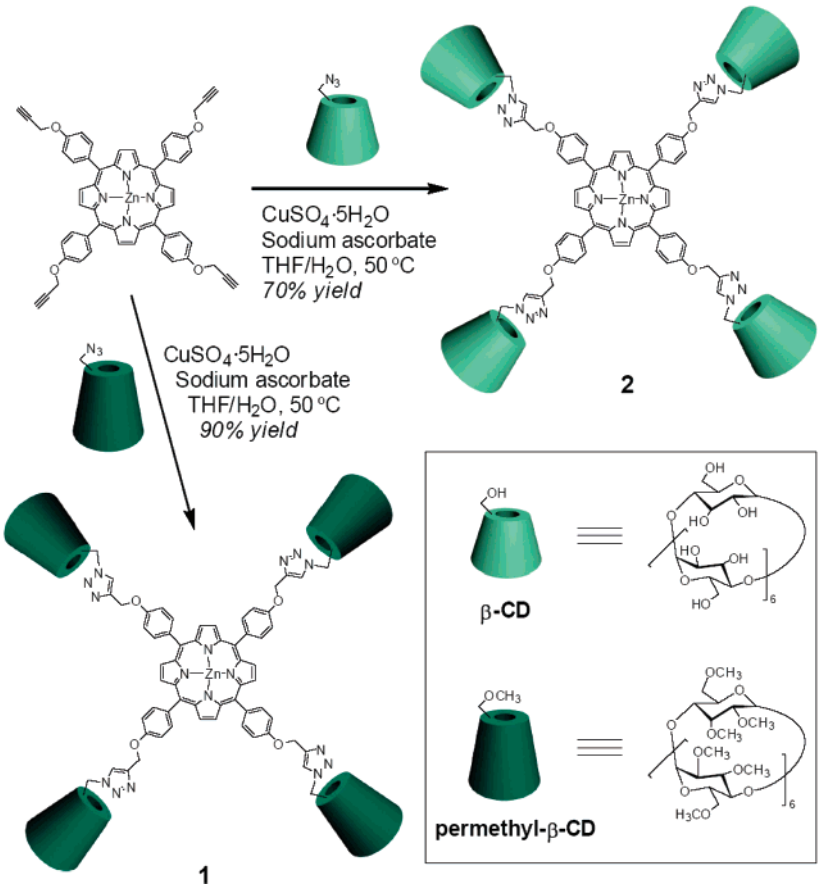

Results and Discussion

Synthesis. The reactions of 5,10,15,20-tetrakis(4′-propagyloxyphenyl)-Zn(II)-porphyrin with 6-deoxy-6-azido-permethyl-β-CD and 6-deoxy-6-azido-β-CD in THF/H_2O afforded tetrakis-(permethyl-β-CD)-modified Zn(II) porphyrin (**1**, 90% yield) and tetra-β-CD-modified Zn(II) porphyrin (**2**, 70% yield), respectively, via "click chemistry" (Scheme 1), from which the supramolecular nanoarchitectures were constructed by the complexation of **3** with **2** and **1** in aqueous solution.

TEM, AFM, and SEM Images. Representative TEM, AFM, and SEM images of the aggregate of **2** and **3** are shown in Figure 1(a−c), where we can clearly see the nanorods on the substrates. In the TEM image, the length of the nanorods is more than 100 nm, and there are several parallel fiberlike nanowires with widths of about 2 nm. The AFM image shows two nanorods with heights of 8 nm and lengths of 500 nm and 3 μm, respectively. Similarly, a number of nanorods with lengths of several hundred nanometers are observed in the SEM image. These observations exclude the possibility that all intermolecular interactions between four CD cavities in **2** and four sulfonic acid groups in **3** occur. The self-assembly process should take place between two opposite CD moieties of **2** and two opposite phenylsulfonic acid groups.

Surprisingly, the nanoarchitectures formed by the complexation of **1** with **3** in aqueous solutions are distinctly different from those described above. Both the TEM and the AFM images show two-dimensional netlike aggregates (Figure 1d,e). The SEM image in Figure 1f shows the surface morphologies of the aggregates. The latter are the flakelike structures with many holes, which is consistent with the observations from TEM and AFM. With the fact that both **1** and **2** contain the same porphyrin core, and the only difference between the two is the outer CD moieties (one is a permethylated CD and the other is a native one), the formation of these two distinct nanoarchitectures led us to investigate the origin of the difference.

NMR Spectra of 1 and 2. We first investigated the conformation of **1** and **2** in aqueous solution as well as in organic solvents by NMR spectroscopy. Compound **1** has high solubility in both chloroform and aqueous solution, while **2** is soluble in DMSO and in aqueous solution. For this reason, all NMR experiments were performed in all three solvents. As shown in Figure 2, the ^{1}H NMR spectrum of **1** in $CDCl_3$ is completely different from that in D_2O. In $CDCl_3$, there are four groups of signals (δ = 8.95, 8.14, 7.95, and 7.37 ppm) in the low field region. They are assigned to the protons of the pyrrole rings, the *ortho*-phenyl moieties, the triazole rings, and the *meta*-phenyl moieties, respectively (Supporting Information). No protons are found in the high field region below 2.5 ppm. Interestingly, the peaks corresponding to the protons of the pyrrole rings and the phenyl moieties are split into several different subsets in D_2O, with accompanying moderate peak shifts. Many new proton signals also appear in the range of −0.5 to 2.0 ppm (Figure 2b). These observations are very similar to those made in the case of 10,20-bis(3,5-dicarboxylatophenyl)-5,15-diphenylporphyrin-permethyl-β-CD conjugate,[9] which allows us to assign these upfield-shifted protons to the secondary OCH_3 groups of the CD moieties.[9] This assignment is validated by the hetero-

(9) Nishiyabu, R.; Kano, K. *Eur. J. Org. Chem.* **2004**, 4985−4988.

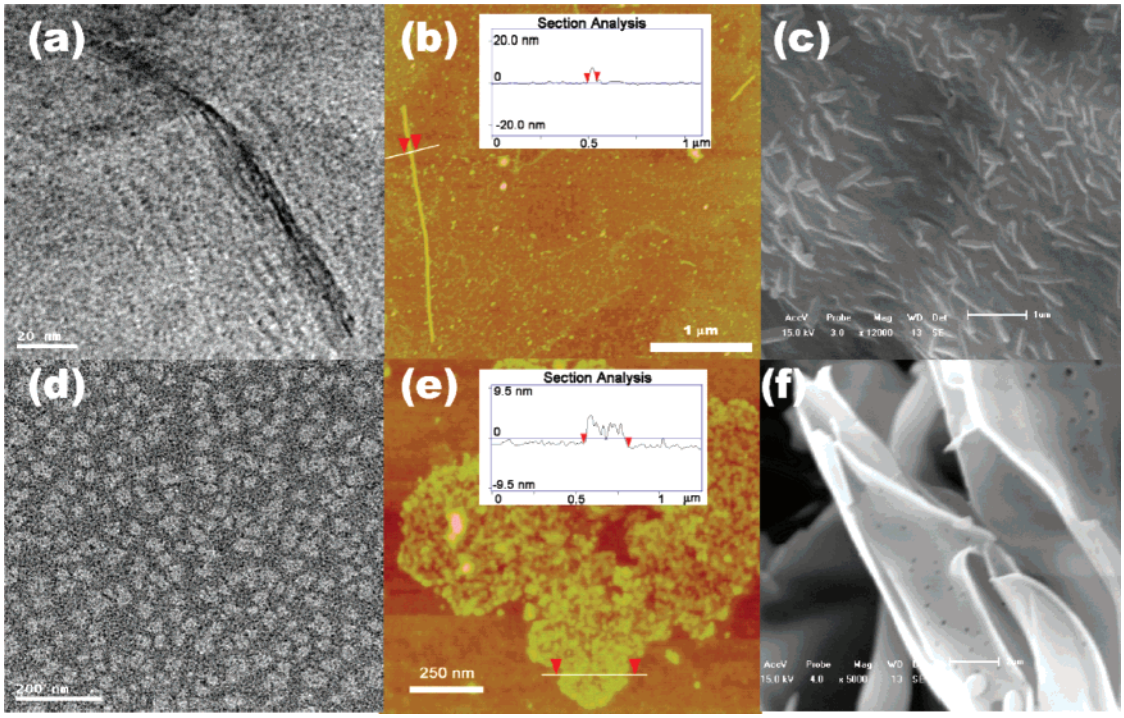

Figure 1. TEM (a and d), AFM (b and e), and SEM (c and f) images of the nanoarchitectures formed upon complexation of **3** with **2** (a−c) and **1** (d−f).

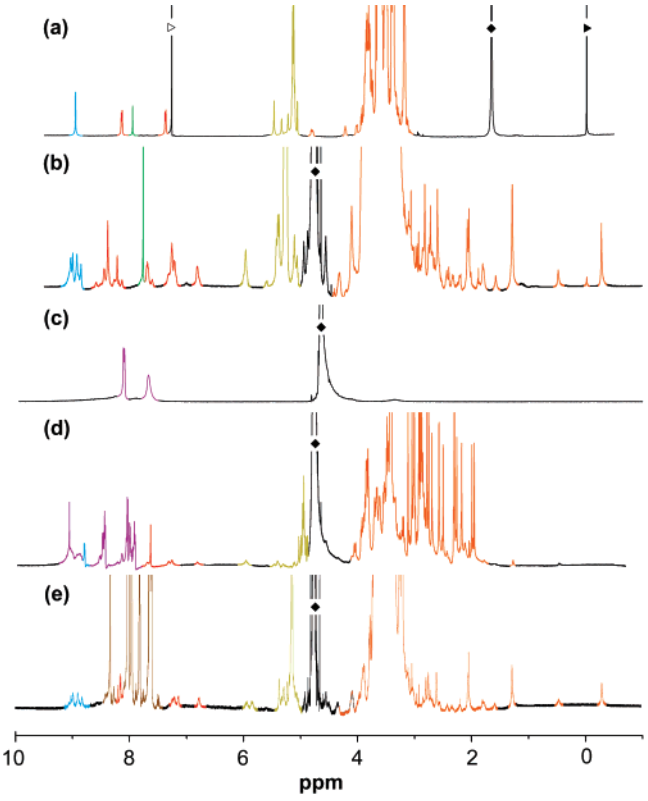

Figure 2. ^{1}H NMR spectra of (a) **1** in $CDCl_3$, (b) **1** in D_2O, (c) **3** in D_2O, (d) **1** (0.60 μM) with **3** (2.44 μM) in D_2O, and (e) **1** (0.60 μM) with 2-NS (21.7 μM) in D_2O. Filled side triangle, open side triangle, and filled diamonds represent TMS or residual solvent peaks in $CDCl_3$ and D_2O.

nuclear multiple bond coherence (HMBC) spectrum of **1** in D_2O (Supporting Information). Furthermore, the NOESY spectrum of **1** in D_2O (Supporting Information) exhibits the cross-peaks between the protons of the secondary OCH_3 with those of the porphyrin's pyrrole and the phenyl moieties, clearly indicating that the secondary sides of CDs are located near the pyrrole and phenyl groups. That means that some CDs in **1** include the porphyrin part by rotating 360° around the pivot glucopyranose unit in the methylated CD. Considering the steric hindrance of CDs around the porphyrin core,[6c] we conclude that only the two CD moieties of **1** at opposite positions intramolecularly include the porphyrin part in aqueous solution. The schematic representations of the partial self-inclusion by a full rotation of the permethylated glucopyranose units and the conformational changes of **1** in chloroform and water are illustrated in Figure 3.

Just as observed for **1** in $CDCl_3$, the aromatic portions in the ^{1}H NMR spectrum of **2** in DMSO-d_6 also exhibit four groups of signals at $\delta = 8.85$, 8.36, 8.11, and 7.48 ppm. However, the triazole protons of **2** shift downfield to a greater extent to 8.36 ppm than those of **1** (7.95 ppm), which suggests that the triazole groups are included inside the cavity of CD. On the other hand, there are ^{1}H signals in the high field region below 1.5 ppm and ^{13}C ones below 40 ppm, and the correlation peaks are observed between these proton signals in the high field region and the ^{13}C signals in the heteronuclear multiple quantum coherence (HMQC) spectrum of **2**. Its HMBC spectrum suggests that these high field signals are assigned to the CD's H-2 and H-3 protons (Supporting Information). Therefore, one can deduce reasonably that the secondary face of some CDs in **2** includes the porphyrin part. The 2D NMR spectrum of **2** in DMSO-d_6 shows strong NOE cross-peaks between the triazole protons and the CD's H3 and H5, and also weak cross-peaks of the pyrrole and phenyl protons with the CD's H-3. These observations unambiguously indicate that the hydrophobic cavity of CD intramolecularly includes the triazole group from the wide-opening secondary face. The attempt to obtain a clear-cut spectrum of **2** in D_2O was not successful as the four groups of the peaks as well as those in CD become broad as the percentage of D_2O increases. This signal broadening may be attributed to the fast equilibrium

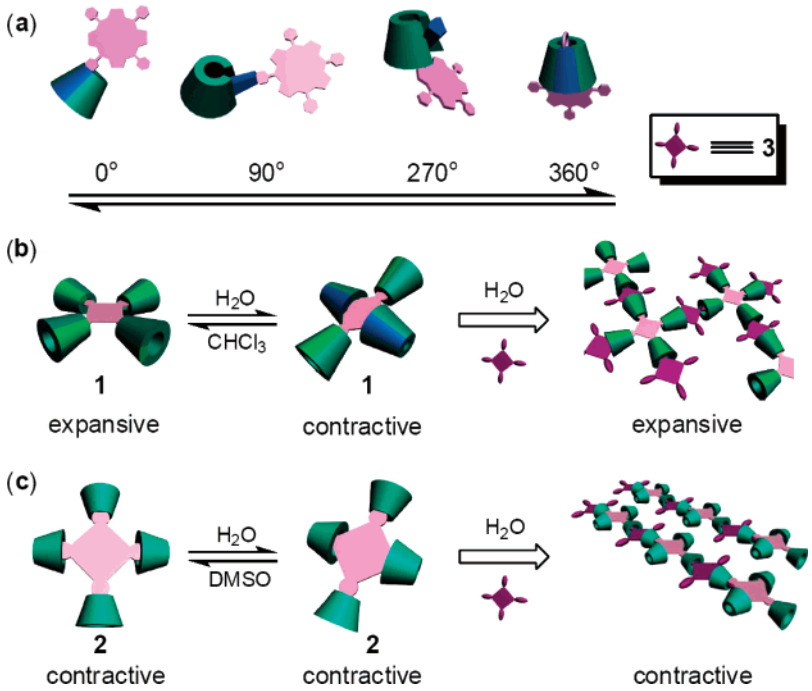

Figure 3. Schematic representation of (a) the partial self-inclusion caused by a full rotation of the pivotal permethylated glucopyranose units, (b) the conformational switching of **1** in chloroform and in water, and the corresponding assembly mode with **3**, and (c) the conformational switching of **2** in dimethylsulfoxide and in water, and the corresponding assembly mode with **3**.

shift of the CD moiety between the triazole and phenyl moieties, as illustrated in Figure 3c. With the information of **2** in DMSO and H_2O, we can make the reasonable deduction that the CD moieties in **2** always exist in the intramolecular self-inclusion mode in both DMSO and H_2O. Similar to that of **1**, only two opposite CD moieties of **2** are thought to adopt the self-included conformation, and the other two remain free, as illustrated in Figure 3c. We also carried out molecular dynamics simulations, using the Dreiding force field,[10] to compare the stabilities of the two self-included conformations of **2** (i.e., the oppositely versus adjacently capped). The calculation results indicate that the oppositely capped conformer is energetically more stable than the adjacently capped one, for which the severe steric hindrance between the two adjacent self-including CDs is responsible. This contractive conformation of **2** probably comes from the preferential threading of only two opposite side chains of the tetrakis(propargyloxyphenyl)porphyrin through the 6-azido-CD cavity in THF/H_2O solution before the click cyclization. In this way, only the remaining two CDs are active and rod array can be formed upon interaction with **3**.

Microcalorimetric Titration. It is well known that adamantane derivatives nicely fit into the cavities of both native and permethylated β-CDs in a 1:1 stoichiometric ratio.[11] Therefore, we chose 1-adamantaneacetic acid (1-AD) as the reference guest to measure the number of the "inert" cavities of **1** and **2** in aqueous solution by titration calorimetry. The microcalorimetric titration experiments gave typical titration curves for 1:2 stoichiometry for the complexations of both **1** and **2** with 1-AD. The stoichiometries of complexation (*n* value) obtained from the curve fitting of the binding isotherm are very close to 2, clearly indicating that the majority of the inclusion complexes of **1** and **2** with 1-AD is 1:2 and there are two free CD cavities in each porphyrin-CD conjugate.

Table 1. Complex Stoichiometry (*n*), Stepwise Binding Constants (K_S/M^{-1}), Enthalpy (ΔH/kJ·mol^{-1}), and Entropy Changes ($T\Delta S$/kJ·mol^{-1}) for 1:*n* Inclusion Complexation of **2** or **1** with 1-AD/**3** in Aqueous Phosphate Buffer Solutions of pH 7.0 at 298 K

host	guest	n	K_S[a]	$-\Delta H$	$T\Delta S$
2	1-AD	1.9	$(8.7 \pm 0.3) \times 10^4$	29.0 ± 0.2	-0.9
1	1-AD	2.1	$(1.4 \pm 0.3) \times 10^3$	16.1 ± 0.5	0.4
2	**3**	1.0	$(4.2 \pm 0.7) \times 10^4$	33.1 ± 2.2	-6.7
1	**3**	2.0	$(2.7 \pm 0.4) \times 10^7$	70.6 ± 1.3	-7.0

[a] Values corresponding to the one set of binding sites model.[13] This model will work for any number of sites (*n*), if all sites have the same K_S.

Although there are four phenylsulfonic groups in **3**, only the opposite two of them can interact with the cavity of CD.[6c,7a,c,12] When **3** was used as a guest in the microcalorimetric experiments, the anticipated 1:1 (*n*/*n*) stoichiometry was observed for the inclusion complexation with **2**, while somewhat unexpected 1:2 (*n*/2*n*) stoichiometry was obtained upon complexation of **1**, with a binding constant of 2.67×10^7 M^{-1} (Table 1). One reasonable explanation for this unusual stoichiometry is that the very strong affinity of the CD cavity of **1** with the phenylsulfonic group of **3** induces the turnover of the pivotal permethylglucopyranose unit to recover the original position in CD, which leads **1** to the "expansive mode" in aqueous solution (Figure 3b). As a result, all four CD cavities in **1** become available for the inclusion complexation with **3** possessing two binding sites,[6c,7a,c,12] resulting in the 1:2 (*n*/2*n*) stoichiometry. Both of

(10) Mayo, S. L.; Olafson, B. D.; Goddard, W. A., III. *J. Phys. Chem.* **1990**, *94*, 8897−8909.
(11) (a) Miyauchi, M.; Hoshino, T.; Yamaguchi, H.; Kamitori, S.; Harada, A. *J. Am. Chem. Soc.* **2005**, *127*, 2034−2035. (b) Charlot, A.; Heyraud, A.; Guenot, P.; Rinaudo, M.; Auzely-Velty, R. *Biomacromolecules* **2006**, *7*, 907−913.
(12) Bonchio, M.; Carofiglio, T.; Carraro, M.; Fornasier, R.; Tonellato, U. *Org. Lett.* **2002**, *4*, 4635−4637.
(13) Tellini, V. H. S.; Jover, A.; García, J. C.; Galantini, L.; Meijide, F.; Tato, J. V. *J. Am. Chem. Soc.* **2006**, *128*, 5728−5734.

the 1:1 binding mode for the inclusion complexation of **2** with **3** and the 1:2 binding mode for **1** with **3** were subjected to fluorescence titration studies (Supporting Information), which further confirmed the results of the above microcalorimetric experiments.

NMR Spectra of 1 in the Presence of 3. To further validate the conclusions concerning the conformation change of **1** in the presence of **3**, NMR studies of **1** in the presence of **3** and sodium 2-naphthalenesulfonate (2-NS)[14] were performed in D_2O. As seen from Figure 2b−e, the original single signals in the range of −0.5 to 2.0 ppm disappear upon the addition of **3**, while they still remain upon the addition of excess 2-NS (Figure 2e). The 2D NMR spectrum of **1** in the presence of **3** (Supporting Information) shows that **3** is included in the cavities of the permethyl-CDs, and the NOE cross-peaks between the CD's H3 and H5 and the aromatic protons in **1** disappear. These observations confirm the conformational change of **1** in aqueous solution from a contractive mode to an expansive mode upon the inclusion complexation with **3**. Consequently, the formation of the network aggregates of **1**−**3** is a natural process.

Conclusion

Two distinctly different nanoarchitectures with alternating porphyrin and CD arrays have been synthesized through the intermolecular inclusion complexation of guest **3** with structurally resembling tetrad host **1** and dyad host **2**, respectively. From the comparative studies in different solutions, we elucidated the mechanisms that result in the transition of nanorods to network aggregates. (a) Host **1** exists in an expansive mode in chloroform and can be reversed to a contractive mode through a 360° rotation of the permethylated glucopyranose units while dissolved in water. Upon the addition of excess **3**, the two rotated CD moieties are pulled out from the porphyrin core to the original expansive mode. As a result, all four permethyl CD moieties can include guest **3** to form a network aggregate. (b) Host **2** always exists in a contractive mode in both dimethylsulfoxide and water. The addition of excess **3** cannot induce the two intramolecular self-inclusion CD cavities to become free. In this case, **3** only can interact with the other two free CD moieties of **2** and form nanorod-like aggregates. Furthermore, we concluded that the complexation strength of the porphyrins toward the CDs is crucial to activating potential building sites of a molecular building block. This new observation will allow us to rationally design and construct a wide range of supramolecular nanoarchitectures by carefully choosing the right combinations of molecular building blocks.

Experimental Section

Materials. β-Cyclodextrin was purchased from Wako. Propargyl bromide solution (80 wt % in toluene) was purchased from Acros Organics. Sodium ascorbate was purchased from Amresco Company. 6-Deoxy-6-azido-permethyl-β-CD[15] and 6-deoxy-6-azido-β-CD[15a] were prepared according to the literature procedure. Other chemicals and solvents were commercially available. DMF and DMSO were distilled from calcium hydride. Column chromatography was performed on silica gel (200−300 mesh) or Sephadex G-25.

(14) There are two reasons for using 2-NS instead of 1-AD: (1) proton signals of 1-AD will overlap with the unique six singlet signals of **1** in ^{1}H NMR spectrum, and (2) 2-NS has a binding ability with CD similar to that of 1-AD.

(15) (a) Hocquelet, C.; Blu, J.; Jankowski, C. K.; Arseneau, S.; Buisson, D.; Mauclaire, L. *Tetrahedron* **2006**, *62*, 11963−11971. (b) Reetz, M. T.; Waldvogel, S. R. *Angew. Chem., Int. Ed.* **1997**, *36*, 865−867.

Measurements. ^{1}H NMR spectra were recorded on a Varian Mercury Plus 400 MHz spectrometer in D_2O and DMSO-d_6 using tetramethylsilane as an internal reference. The ^{1}H NMR data are reported as follows: chemical shift (δ in ppm), multiplicity (bs = broad singlet, bt = broad triplet, bm = broad multiplet, s = singlet, d = doublet, t = triplet, q = quartet, m = multiplet), and peak integrals. ^{1}H NMR peaks were assigned from 2D COSY spectra. 2D ROESY spectra were recorded on a Varian 300 MHz spectrometer. ^{13}C NMR, HMQC, and HMBC experiments were carried out on a Bruker 600 MHz NMR spectrometer. Positive-ion matrix-assisted laser desorption ionization mass spectrometry was performed on an IonSpec QFT-MALDI MS. UV−vis spectra were recorded in a conventional quartz cell (10 mm) at 25 °C on a Shimadzu UV2401 spectrophotometer. Fluorescence spectra were recorded on a JASCO FP750 or Edinburgh Analytical Instruments FL900CD (Edinburgh Instruments) spectrometer in a 10-mm quartz cell at 25 °C.

TEM Measurements. A 50-μL portion of sample solution was dropped onto a copper grid. The grid was then air-dried. The samples were examined by a high-resolution TEM (Philips Tecnai G2 20 S-TWIN microscope) operating at an accelerating voltage of 200 keV.

AFM Measurements. A 10-μL portion of sample solution was dropped onto newly clipped mica and washed with 1 mL of distilled water and then air-dried. The samples were examined using an AFM (Veeco Company, Multimode, Nano IIIa) in tapping mode in the air at room temperature.

Microcalorimetric Titration. All the microcalorimetric titration experiments were performed on a Microcal VP-ITC titration microcalorimeter, which permits us to simultaneously determine the enthalpy change ($\Delta H°$) and the equilibrium constant (K_S) from a single titration curve. The sample cell volume was 1.4227 mL. Each titration experiment included 25 successive injections. All solutions were degassed and thermostated using a ThermoVac accessory before the titration experiments were performed.

ORIGIN software (Microcal) was used for the calculation of binding constant (K_S) and standard molar reaction enthalpy ($\Delta H°$) from each titration curve with a standard derivation on the basis of the scattering of data points in a single titration experiment. The binding stoichiometry (n) was also given as a fitting parameter. From the binding constant (K_S) and molar reaction enthalpy ($\Delta H°$) obtained, one can calculate the standard Gibbs free energy of binding ($\Delta G°$) and the entropy change ($\Delta S°$).

Preparation of 5,10,15,20-Tetrakis(4′-propargyloxyphenyl)-Zn-(II)-porphyrin. 4-(Prop-2-ynyloxy)benzaldehyde (3.2 g) was dissolved in 500 mL of propionic acid with stirring. The resulting solution was heated to reflux, and then newly pyrrole (1.3 g) was added. The solution turned to dark purple rapidly. The solution was cooled down after 3 h, and propionic acid was removed under reduced pressure. Triethylamine (5 mL) was then added to the residue, and the mixture was precipitated by adding methanol (200 mL). The precipitate was collected by filtration and washed by methanol twice (50 mL). The crude purple product was purified by silica gel chromatogram using dichloromethane as eluent. The final 5,10,15,20-tetrakis(4′-propargyloxyphenyl)-porphyrin was obtained in 13% yield as a purple powder. ^{1}H NMR ($CDCl_3$, 300 MHz, ppm): δ 8.79 (s, 8H), 8.08 (d, 8H), 7.30 (d, 8H), 4.92 (d, 8H), 2.63 (t, 4H), −2.84 (2H). ESI-MS: m/z 830.8 (M^+). After 5,10,15,20-tetrakis-(4′-propargyloxyphenyl)-porphyrin was dissolved in chloroform/methanol (v/v = 1:1) solution, 10 times zinc acetate in methanol was added. The solution was refluxed for 3 h and then cooled and dried. Choloform (20 mL) was added in the residue and then filtrated to remove the insoluble ones. The filtrate was then dried to get the final product. ESI-MS: m/z 892.5 (M^+).

Preparation of 1. To a solution of 5,10,15,20-tetrakis(4′-propargyloxyphenyl)-Zn(II)-porphyrin (200 mg, 0.223 mmol) in THF (20 mL), 6-deoxyl-6-azido-permethyl-β-CD (2 g, 1.39 mmol) in THF (20 mL) was added with stirring. To the resulting solution, $CuSO_45H_2O$ (360 mg) and then sodium ascorbate (850 mg) dissolved in water (15 mL)

were added. The color of the mixture turned brown immediately and then dark purple in a few minutes. The solution was heated at about 50 °C for 48 h. The mixture was then dried under reduced pressure, and the residue was dissolved in chloroform. Insoluble precipitates were removed by filtration, and the filtrates were dried and further purified by flash column chromatography using a chloroform−methanol (v/v = 30:1) eluent to give the product as a violet powder in 90% yield. ^{1}H NMR ($CDCl_3$, 600 MHz, ppm): δ 8.95 (s, 8H), 8.14 (d, 8H), 7.95 (d, 4H), 7.37 (d, 8H), 5.47 (s, 8H), 5.23−5.06 (m, 28H), 4.81 (m, 4H), 4.22−3.13 (m, 404H). Anal. Calcd for $(C_{304}H_{472}N_{16}O_{140}Zn)(H_2O)_{36}(DMF)_2$: C, 49.97%; H, 7.55%; N, 3.38%. Found: C, 49.50%; H, 7.49%; N, 3.34%. MALDI-MS: m/z 6651 (M^+).

Preparation of 2. Almost the same procedures described above were employed. The crude product obtained was further purified by HPLC (reversed phase) with a water−acetonitrile (v/v = 72:28) eluent, and the collected fraction was freeze-dried to obtain violet powder in 70% yield. ^{1}H NMR (DMSO-d_6, 600 MHz, ppm): δ 8.85 (s, 8H), 8.36(s, 4H), 8.11(m, 8H), 7.48 (m, 8H), 5.94−5.75 (m, 56H), 5.42 (m, 8H), 5.11−4.52 (m, 56H), 4.14−4.12 (m, 8H), 3.66 (m, 76H, overlapped with the DOH peak), 3.36 (m, 70H), 1.23 (m, 10H), 0.86 (m, 4H). Anal. Calcd for $(C_{224}H_{312}N_{16}O_{140}Zn)(H_2O)_{23}(DMF)_3$: C, 45.37%; H, 6.19%; N, 4.31%. Found: C, 45.18%; H, 5.86%; N, 4.49%. MALDI-MS: m/z 5471 $(M + H)^+$.

Preparation of Assemblies. Compound **3** solutions in different molar ratios were added with stirring to aqueous solutions of **1** (or **2**). After being stirred for 1 h, the solutions were freeze-dried to give the final assemblies as purple powders, which were further characterized by NMR, AFM, TEM, and SEM.

Acknowledgment. This work was supported by the 973 Program (2006CB932900), NNSFC (Nos. 90306009, 20421202, and 20572052), and the Program for New Century Excellent Talents in University (NCET-05-0222). We thank the reviewers for their valuable comments and suggestions regarding the revision. We also thank Prof. Yoshihisa Inoue at Osaka University (Japan) for his suggestions and discussions, and Prof. Vernon D. Parker at Utah State University and Dr. Xiaopeng Bai at Helicos BioSciences Corporation for assistance in the preparation of this manuscript.

Supporting Information Available: ^{1}H NMR and MALDI-MS spectra of **1** and **2**; ^{13}C NMR, HMQC NMR, and HMBC NMR spectra of **1**; ^{13}C NMR, HMQC NMR, HMBC NMR, and 2D NOESY spectra of **2** and **1** with/without **3**; electronic absorption spectra; schematic representation of **2**; fluorescence titrations of **1** and **2** in the presence of increasing amounts of **3**; and ITC titration curves. This material is available free of charge via the Internet at http://pubs.acs.org.

JA075981V